

## Small reversible axial-strain window for the critical current of a high performance Nb<sub>3</sub>Sn superconducting strand

Xi Feng Lu, Stephen Pragnell, and Damian P. Hampshire<sup>a)</sup>

Superconductivity Group, Physics Department, Durham University, Durham, DH1 3LE, United Kingdom and Grenoble High Magnetic Field Laboratory, B.P. 166, 38042 Grenoble Cedex 9, France

(Received 25 July 2007; accepted 4 September 2007; published online 28 September 2007)

The engineering critical current density ( $J_C$ ) of a Nb<sub>3</sub>Sn restacked-rod-process superconducting strand is reported as a function of magnetic field ( $B \leq 28$  T), applied axial strain ( $-0.9\% \leq \varepsilon_A \leq 0.2\%$ ), and temperature ( $4.2 \text{ K} \leq T \leq 14 \text{ K}$ ). Although the strain tolerance of  $J_C$  is similar to other strands, the strain range over which  $J_C$  is reversible is limited in both tension and compression. Samples were partially damaged when the intrinsic strain ( $\varepsilon_I$ ) was increased from  $-0.74\%$  to  $-0.97\%$  in compression and grossly damaged when  $\varepsilon_I$  was only  $0.13\%$  in tension. © 2007 American Institute of Physics. [DOI: 10.1063/1.2789696]

The International Thermonuclear Experimental Reactor (ITER) is one of the biggest scientific projects in the 21st century. The ITER requirement for more than 500 tons of Nb<sub>3</sub>Sn strands has provided an enormous impetus for developing high performance strands since the 1990s.<sup>1</sup> One can consider the Nb<sub>3</sub>Sn strands available in two categories: Firstly, there are bronze-route and advanced internal-tin strands that have sufficiently low ac losses for fusion (ITER) applications but the engineering  $J_C$  (defined as the critical current divided by the total cross-sectional area of the strand) is also low, typically  $300\text{--}600 \text{ A mm}^{-2}$  at  $4.2 \text{ K}$  and  $12 \text{ T}$  (non-Cu  $J_C \sim 800\text{--}1200 \text{ A mm}^{-2}$ ),<sup>1</sup> and secondly, restacked-rod-process (RRP) internal-tin strands and powder-in-tube strands for high-energy physics and NMR applications that have ac losses that are too high for ITER but provide very high  $J_C$  values of  $\sim 1200 \text{ A mm}^{-2}$ .<sup>1,2</sup> The bronze-route and the two types of internal-tin strands are shown in Fig. 1,<sup>3-5</sup> including the high  $J_C$  RRP strand that is the subject of this letter.<sup>2</sup> We report detailed  $J_C(B, T, \varepsilon)$  data as a function of field ( $B$ ), temperature ( $T$ ), and axial strain ( $\varepsilon$ ) for the RRP strand (and the associated scaling law) as well as a strain range (or window) beyond which the strand can be damaged in either tension or compression.

The  $J_C(B, T, \varepsilon)$  measurements were performed using our purpose-built  $J_C(B, T, \varepsilon)$  probe.<sup>6</sup> At particular values of magnetic field, temperature, and strain, measurements are made of the voltage across sections of the sample as a function of the current through it.  $J_C$  (or  $I_C$ ) is defined at an electric field criterion of  $10 \mu\text{V m}^{-1}$ . Three RRP  $0.81 \text{ mm}$  diameter Nb<sub>3</sub>Sn strands with 91 subelements were reacted in a high homogeneity tube furnace under an argon atmosphere using the heat treatment:  $210 \text{ }^\circ\text{C}$  for 48 h,  $400 \text{ }^\circ\text{C}$  for 48 h, and  $640 \text{ }^\circ\text{C}$  for 60 h (all the ramp rates were  $10 \text{ }^\circ\text{C h}^{-1}$ ). Samples S1 and S3 were reacted together and sample S2 by itself. Samples S1 and S2 were measured using the superconducting magnet ( $B < 15 \text{ T}$ ) in Durham. Sample S3 was measured in Grenoble in magnetic fields up to  $28 \text{ T}$ . More details about the experimental apparatus and techniques can be found elsewhere.<sup>6,7</sup>

Significant time and effort can be expended in identifying the strain range over which  $J_C$  remains reversible for a

strand. We use four tests to assess whether the strand has been damaged and hence, whether the  $J_C$  data are reliable. Initially, we measure  $I_C$  at  $4.2 \text{ K}$  and a few magnetic fields to confirm the specifications of the manufacturer. For the RRP strand,  $I_C$  was  $586 \text{ A} \pm 3\%$  at  $4.2 \text{ K}$ , and  $12.25 \text{ T}$  (cf. Fig. 1) which is within 1% of the manufacturer's nominal value. Throughout the experiment, we check: the homogeneity of the strand—typically five different sections of the strand are measured, each approximately  $20 \text{ mm}$  long; the (zero-resistance) base line of the  $V$ - $I$  data, to ensure that it is flat to within the noise of our measurement (typically a few nanovolts); and the reversibility of the sample, by measuring whether or not  $J_C(B, T, \varepsilon)$  at zero applied strain is reversible to within a few percent—since high compressional strains cause some components of the matrix and the spring to plastically deform.<sup>8</sup>

Figure 2 shows good agreement between the  $J_C$  (and  $I_C$ ) values as a function of magnetic field at  $4.2 \text{ K}$  under compressive strain measured for all three RRP samples studied. For samples S1 and S2, once the applied compressive strain was increased beyond  $-0.67\%$ , the  $J_C$  of the strands were not homogeneous, consistent with partial damage. Homogeneity

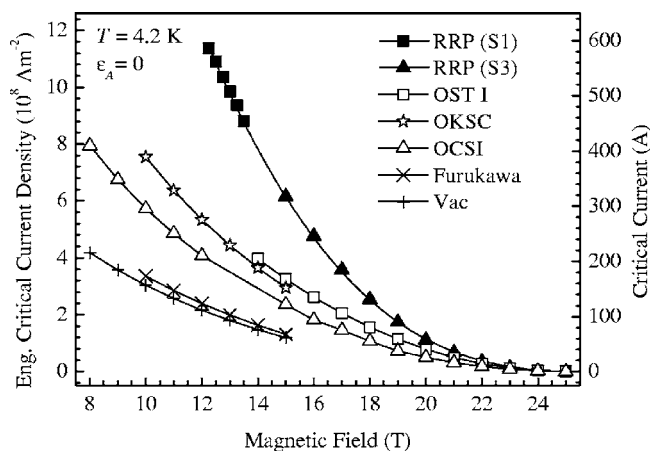


FIG. 1. Engineering critical current density  $J_C$  (and critical current  $I_C$ ) vs magnetic field for Nb<sub>3</sub>Sn strands made by different manufacturers. The Vac and Furukawa are bronze-route strands. OCSI, OKSC, and OST I are advanced internal-tin strands (see Refs. 3–5). Samples S1 and S3 are the RRP strand presented in this work.

<sup>a)</sup>Electronic mail: d.p.hampshire@durham.ac.uk

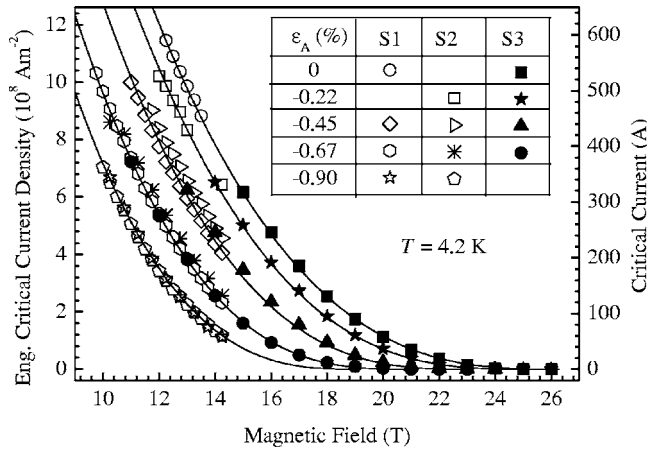


FIG. 2. Engineering critical current density (and critical current) as a function of magnetic field at 4.2 K for samples S1, S2, and S3. The lines are provided by the scaling law.

tests on different sections showed that increased compressive strain down to  $\epsilon_A - 0.9\%$  caused progressively more damage. As the damage increased, we found that some sections began to quench over some limited field ranges so that  $I_C$  could not be measured. Figure 3(a) is a plot of  $J_C$  (and  $I_C$ ) as a function of applied strain at 4.2 K for S1 for magnetic fields at and below 14.25 T with field increments of 0.25 T. At  $\epsilon_A \sim -1.1\%$ , a shaft in the probe failed which prevented further measurements on S1. For sample S2, after the compressive measurements at 4.2 K, measurements were made at 8 and 12 K. Further compressive measurements (at these higher temperatures) caused further damage and a reduction in  $I_C$  of about 15% from the original values. Then, tensile strain was applied. At  $\epsilon_A \sim +0.2\%$  gross damage occurred—one section was completely resistive, others had very low  $J_C$  values, and some were not measurable (i.e., quenched). Given that S1 and S2 were both damaged in compression beyond  $-0.67\%$ , we restricted measurements on S3 at 4.2 K to  $-0.67\% < \epsilon_A \leq 0\%$ . Good homogeneity and flat base lines for the  $V-I$  data were found. Then, variable temperature measurements were made at 8, 10, and 14 K over the same compressive range. At  $-0.67\%$ , one of the five sections for S3 was damaged although the others remained reversible. Figures 3(b) and 3(c) show  $J_C$  values for S3 at 4.2 and 8 K. As with S2, once  $\epsilon_A$  was increased (in tension) to  $\sim +0.2\%$ , S3 was seriously damaged. Hence, we conclude that all three samples showed evidence for partial damage when the applied compression was increased from  $-0.67\%$  to  $-0.9\%$  and the two samples measured in tension showed gross damage at  $\sim +0.2\%$ . We confirm that gross damage occurs on applying a small tension to these strands, as observed independently by two other groups,<sup>9</sup> and report a reversibility limit in compression. These strain limits are also consistent with a metallographic

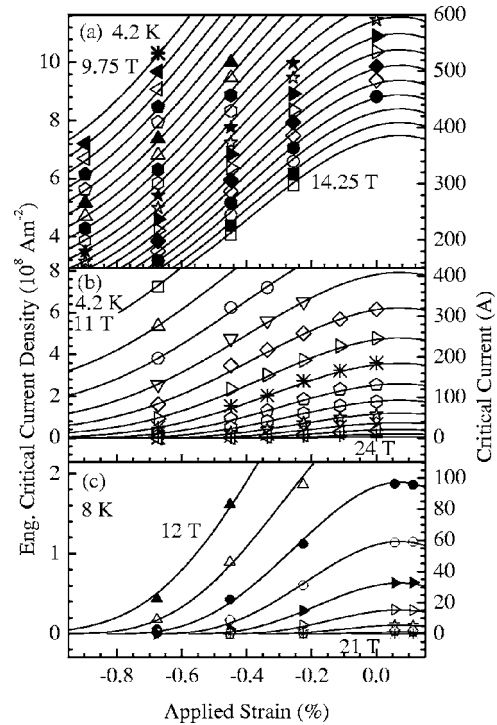


FIG. 3. Engineering critical current density (and critical current) as a function of applied strain at 4.2 and 8 K. (a) Sample S1 in magnetic fields from 14.25 to 9.75 T in increments ( $\Delta B$ ) of 0.25 T at 4.2 K. [(b) and (c)] Sample S3 at 4.2 and 8 K ( $\Delta B = 1$  T), respectively. The lines are provided by the scaling law.

study<sup>10</sup> on similar strands that concluded that at 0.5% bending strain, there was significant evidence for breakage in tension but little if any evidence for cracking in compression.

From the reversible data obtained on samples S1 and S3, we have parametrized  $J_C(B, T, \epsilon)$  using a scaling law proposed previously<sup>8</sup> which is based on combining microscopic theory with phenomenological theory. Initially, the data at temperatures above 4.2 K, which include data at strains above and below the peak in  $J_C$ , were used to obtain an accurate value of  $\epsilon_M$ . Then, a global fit to all the data provided the best-fit values for the other free parameters which are all given in Table I (parameters in bold are not varied in the fitting procedure).<sup>8</sup> Since  $J_C$  peaks when  $\epsilon_A = \sim 0.07\%$ , the small reversible strain window can be expressed in terms of an intrinsic (rather than applied) strain window of  $-0.74\%$  to  $+0.13\%$  where the intrinsic strain is defined to be zero when  $J_C$  reaches its peak value. To a good approximation, the normalized strain tolerance of  $J_C$  is similar in RRP strands to  $Nb_3Sn$  strands made by other fabrication routes—indicated by the good fits obtained using the scaling law and the near-universal behavior of the normalized zero-temperature effective upper critical field.<sup>8</sup> This is consistent

TABLE I. Scaling law parameters for the RRP strand derived from variable strain, field, and temperature data. The four parameters in bold were not varied in the fitting procedure (see Ref. 8).

$p$	$q$	$n$	$\nu$	$w$	$u$	$\epsilon_M$ (%)
1.0404	2.913	<b>2.500</b>	<b>1.500</b>	<b>2.200</b>	<b>0</b>	0.0722
$A(0)$ ( $A m^{-2} T^{3-n} K^{-2}$ )	$T_C^*(0)$ (K)		$B_{C2}^*(0,0)$ (T)	$c_2$	$c_3$	$c_4$
$1.493 \times 10^8$	16.90		30.20	-0.6362	-0.4346	-0.0578

with attributing the strain tolerance of  $J_C$  primarily to the strain tolerance of the fundamental critical superconducting parameters (and that the porosity and voids present in RRP strands have little effect).<sup>8</sup>

In the RRP strands, the subelements have a very different structure to both bronze-route materials and advanced internal-tin strands because the individual filaments coalesce<sup>2</sup> to form a thick superconducting layer (so the ac losses are high). The RRP strands also have significant porosity both within the Nb<sub>3</sub>Sn layer and the Sn reservoir,<sup>10,11</sup> and this porosity is probably responsible for the crack propagation in the twisted filaments at low tensile and compressive axial strains. The gross changes in  $J_C$  (and gross damage) in tension compared to limited damage in compression is expected, since cracks tend to propagate across the superconducting current path in tension and along the current path in compression. In bronze-route strands, reactions at 1300 bars using hot-isostatic pressing (HIP) produced a significant increase in the tensile strain at which damage first appeared.<sup>12</sup> We conclude that further studies are needed to confirm the range of the small axial-strain window we report in this letter for three RRP samples, where the crack initiation sites are located and whether the strands can be improved, for example, by decreasing the porosity by HIP or strengthening the strand<sup>13</sup> to increase the reversible stress window.

The authors thank A. Vostner, E. Salpietro, E. Mossang, K. Osamura, N. Mitchell, A. Nijhuis, and D. M. J. Taylor. This work was supported by EFDA/ITER, EPSRC, and NEDO (Applied Superconductivity, 2004EA004).

- <sup>1</sup>A. Vostner and E. Salpietro, *Supercond. Sci. Technol.* **19**, S90 (2006).
- <sup>2</sup>S. Hong, M. B. Field, J. A. Parrell, and Y. Z. Zhang, *IEEE Trans. Appl. Supercond.* **16**, 1146 (2006).
- <sup>3</sup>D. M. J. Taylor and D. P. Hampshire, *Supercond. Sci. Technol.* **18**, 297 (2005).
- <sup>4</sup>D. P. Hampshire, D. M. J. Taylor, P. Foley, and S. A. Keys, "Characterisation of Nb<sub>3</sub>Sn and Nb<sub>3</sub>Al strands for Model Coils," Report No. DurSC0601, 2001 (unpublished).
- <sup>5</sup>X. F. Lu, D. M. J. Taylor, E. Mossang, and D. P. Hampshire (unpublished).
- <sup>6</sup>D. M. J. Taylor and D. P. Hampshire, *Supercond. Sci. Technol.* **18**, 356 (2005).
- <sup>7</sup>N. Cheggour and D. P. Hampshire, *Rev. Sci. Instrum.* **71**, 4521 (2000).
- <sup>8</sup>D. M. J. Taylor and D. P. Hampshire, *Supercond. Sci. Technol.* **18**, S241 (2005).
- <sup>9</sup>A. Vostner (private communication); EFDA Magnet Experts Workshop, Barcelona, Spain, 2007.
- <sup>10</sup>M. C. Jewell, P. J. Lee, and D. C. Larbalestier, *Supercond. Sci. Technol.* **16**, 1005 (2003).
- <sup>11</sup>P. J. Lee and D. C. Larbalestier, *IEEE Trans. Appl. Supercond.* **15**, 3474 (2005).
- <sup>12</sup>T. Fukutsuka, T. Horiuchi, Y. Monju, I. Tatara, Y. Maeda, and M. Moritoki, *Adv. Cryog. Eng.* **30**, 891 (1984).
- <sup>13</sup>J. W. Ekin, N. Cheggour, M. Abrecht, C. C. Clickner, M. B. Field, S. Hong, J. A. Parrell, and Y. Z. Zhang, *IEEE Trans. Appl. Supercond.* **15**, 3560 (2005).